Journal of Environmental Chemical Engineering 13 (2025) 118671

Contents lists available at ScienceDirect

Journal of Environmental Chemical Engineering

journal homepage: www.elsevier.com/locate/jece

Biodegradation of carbon materials by environmental peroxidases depends on the type of allotropic form

Tengfei Wang [a], Nandita Dasgupta [b,1], Álvaro Artiga [a], Iwona Janica [a], Juan Antonio Tamayo-Ramos [b,2], Carlos Rumbo [b,*], Alberto Bianco [a,*]

[a] CNRS Immunology Immunopathology and Therapeutic Chemistry UPR 3572 University of Strasbourg ISIS, Strasbourg 67000, France
[b] International Research Centre in Critical Raw Materials-ICCRAM, Universidad de Burgos, Plaza Misael Bañuelos s/n, Burgos 09001, Spain

ARTICLE INFO

Keywords:
Graphene
Single-wall carbon nanotubes
Pichia pastoris
Manganese peroxidase
Horseradish peroxidase
Raman

ABSTRACT

Carbon nanomaterials, possessing unique properties and advantages, exhibit broad application prospects. However, their potential risks to life and the environment have constrained their development. Investigating various degradation strategies can mitigate their adverse effects and expand their applications, particularly within the fields of life and materials sciences. Peroxidases are widely utilized for degradation due to their capability to catalyse the breakdown of various organic compounds. In this study, three peroxidases, namely horseradish peroxidase (HRP), *Pichia pastoris*-expressed Eucodis® peroxidase (EP 13), and manganese peroxidase (MnP), were selected to investigate their effects on the enzymatic biodegradation of different allotropic forms of carbon materials, including graphene and single-wall carbon nanotubes (SWCNT). The obvious increase of defects and decomposition of the structures were demonstrated for graphene by Raman spectroscopy and transmission electron microscope (TEM) after the treatment with these peroxidases. No degradation was instead observed in the enzyme-treated pristine SWCNT. The differences of degradation in two carbon nanomaterials are supposed to result from their distinct physicochemical properties. X-ray photoelectron spectroscopy (XPS) and thermogravimetric analysis (TGA) evidenced that a number of oxygen-containing functional groups are present in graphene, likely providing the catalytic sites for the peroxidase action thus facilitating its degradation, as previously demonstrated using other types of oxidative conditions.

1. Introduction

Graphene and carbon nanotubes (CNTs), two of the most classic allotropes of carbon, have shown excellent performance in many areas since their debut, and countless studies have been dedicated to explore their potentials [10]. For example, graphene, as one type of two-dimensional (2D) materials, holds great promises as gas sensor, due to its unique structural and electrical properties. The graphene with a single layer of atoms has high specific surface to volume ratio and high sensitivity to the change of chemical environment, which are beneficial for molecule capture, the detection of reaction processes, and for the generation of sensitive electrical signals [23]. Besides, graphene is also widely used in the energy storage and biomedical fields, due to its good electrical conductivity, high mechanical strength and good biocompatibility [25,28]. On the other hand, CNTs are 1D nanomaterials that are used, for example as coating or doping additives to provide high mechanical strength and specific functions such as photothermal effect, electric conductivity, corrosion resistance, etc. [2,16]. In addition, the specific properties of CNTs have also attracted the attention of the biomedical field in recent years [9]. For instance, CNTs were dopped into hydrogels based on self-assembled amino acids, endowing the hybrids with a high mechanical strength, a photothermal effect and a near-infrared irradiation-triggered drug release. This design demonstrates that CNTs have great potential in multifunctional tissue engineering application [11].

After few decades of development, the industrial applications of graphene and CNTs are becoming increasingly widespread. However, the potential hazards of carbon nanomaterials to life and the environment have gradually drawn particular attention. Some studies have reported that carbon nanomaterials can induce cytotoxicity and

* Corresponding authors.
E-mail addresses: crumbo@ubu.es (C. Rumbo), a.bianco@ibmc-cnrs.unistra.fr (A. Bianco).
[1] Current address: CSIR-Indian Institute of Toxicology Research, Lucknow 226001, Uttar Pradesh, India.
[2] Current address: Instituto de Agroquímica y Tecnología de Alimentos, IATA, CSIC, Valencia, Spain.

https://doi.org/10.1016/j.jece.2025.118671
Received 26 May 2025; Received in revised form 31 July 2025; Accepted 12 August 2025
Available online 13 August 2025

inflammatory response in living bodies [3,18]. For example, functionalized CNTs have been reported to cross the blood-brain barrier and generate neurotoxicity [5]. Moreover, another worrying issue raised by CNTs is their potential for human pulmonary toxicity, which may cause asbestosis, bronchogenic carcinoma, mesothelioma, pleural fibrosis and pleural plaques due to the asbestos-like fibrous structure [6]. In another study, graphene has shown cytotoxicity in skin fibroblasts by generating ROS and damaging the mitochondria [15]. Due to their industrial development and employment in commercial products for a wide variety of applications, carbon nanomaterial exposure can also exhibit a potentially negative impact on the environment and the ecosystems. Taking industrial CNTs as an example, they can be released in the nature by many routes and after different transformations, CNTs can interact with soils, sediments as well as water, ultimately displaying ecotoxicity to human, animal and microorganisms [21,22].

To overcome or alleviate these problems, the demonstration of carbon nanomaterial degradation was proposed as one of the safe strategies. Many different methods including photodegradation, oxidative degradation and biodegradation were studied and reported [21]. Among them, biodegradation is highly favoured being environmental clean, renewable and not generating secondary pollutants. In previous works conducted by our group, many possible biodegradation processes were studied *in test tube* (using isolated peroxidases) and *in vitro* (using macrophages and neutrophils) using different types of carbon nanomaterials. For instance, different enzymes such as myeloperoxidase and horseradish peroxidase, have been proved to degrade carbon nanomaterials *in tube* [24]. The study on different types of enzymes can help to understand the degradation mechanism at molecular level and provide more options for degradation strategies, while investigating the degradation pathway at cellular level can address the challenges related to the biomedical application of carbon nanomaterials. Some of the immune cells have been found to possess the capacity for the biodegradation of carbon materials. Furthermore, the biodegradation of CNTs and two kinds of graphene (single-layer and few layer) were described in macrophages and neutrophils respectively. Both of them clean the intracellular carbon materials through generating ROS [7,14]. Additionally, a lot of research has been conducted to understand the environmental transformation of carbon nanomaterials, which is meaningful for studying their life cycle and potential risk in ecosystem [22]. Bacterial community in ecosystem also showed the biodegradation capacity for carbon materials. Through the cooperation of multiple microbes such as *Burkholderia kururiensis*, *Delftia acidovorans*, and *Stenotrophomonas maltophilia*, and the co-metabolism with other external carbon sources, acid-treated CNTs can be transformed into CO_2 [26]. Besides, a degradation ability for graphene oxide was also found in insects. Degraded residual materials were detected in the frass of *Yellow mealworms*, which ingested the graphene oxide. Gut microbes in the insect are proved to play a significant role in the degradation process [17].

In this work, the biodegradation of industrial-sourced graphene and SWCNT by three peroxidases, corresponding to horseradish peroxidase (HRP), *Pichia pastoris*-expressed Eucodis® peroxidase (EP 13) and manganese peroxidase (MnP), was investigated. The study of the biodegradability of carbon materials used in products present in the market can help to understand the fate of these materials once released into the environment and seek viable green degradation strategies. HRP has been widely reported about their degradation capacity for carbon materials, and it was used here as a positive control [1,12]. EP 13 is a recombinant peroxidase from natural sources expressed in *Pichia Pastoris*, belonging to the heme-containing peroxidase group categorized as EC 1.11.1.7. This group of peroxidases is widely found in bacteria, fungi and plants, where they exert a fundamental role in the biodegradation of phenolic compounds. MnP is a peroxidase that naturally occurs in the environment, specific to basidiomycetes, which pose a significant ligninolytic capacity and have shown an extensive ability to degrade numerous pollutants and xenobiotics [4,20]. Therefore, EP 13 and MnP were peroxidases found in natural sources and selected to simulate the natural enzymatic conditions that could be found in the environment. They were chosen to study the transformation of the industrial-sourced carbon materials after releasing to the ecosystem, predicting the environmental removal capacity for these different carbon allotropes. The characterization of the carbon materials was first performed to analyse their structure and their physicochemical properties through dynamic light scattering (DLS), transmission electron microscope (TEM), thermogravimetric analysis (TGA) and X-ray photoelectron spectroscopy (XPS). Then, the degree of degradation of these carbon materials was measured by Raman spectroscopy and TEM after 60-day incubation with the three peroxidases. Graphene and SWCNT proved different degradation outcomes, which can be explained by the variations in the physicochemical properties of the two nanomaterials.

2. Materials and methods

2.1. Materials

EP 13 *Pichia pastoris* peroxidase was obtained from Eucodis® Biosciences (EP013, Austria). HRP type VI-salt free powder was bought from Sigma Aldrich (P8375, USA). MnP from white-rot fungus (*Phanerochaete chrysosporium*) was obtained from Sigma Aldrich (93014, USA). Graphene nanoplatelets were provided by Graphene-XT (Bologna, Italy). SWCNT (commercialised as TUBALL™) were provided by OCSiAl Europe Sarl (Luxembourg). Bovine serum albumin (BSA) was bought from Merck Millipore (126579, USA).

2.2. Dispersion of carbon materials

Fifteen mg of graphene or SWCNT were dispersed in 6 mL of 0.5 % BSA water solution. The material solutions were sonicated by tip sonication (Sonics & Materials, VC 505) for 11 min 45 sec with 20 % amplitude and continuous mode, with a power of 10 W.

2.3. Interaction of carbon materials with enzymes

Two-hundreds μL of each pre-dispersed carbon material (1 mg/mL) was added to 800 μL of a specific buffer for each enzyme (PBS for HRP, 50 mM phosphate buffer (PB) pH 5 for EP 13, and 50 mM sodium malonate buffer pH 4.5 for MnP), and the material solutions were sonicated for 2 min. A blank group was set without adding H_2O_2 or the enzymes. The three experimental groups were set by adding 1 mg of each enzyme plus 2 μL of 10 M H_2O_2 and 2 μl of 1 M $MnCl_2$ (only in vials of MnP) in 1 mL of material solution. H_2O_2 was added every day and each enzyme was refreshed every 20 days (adding 1.0 mg of enzyme in 0.4 mL of specific buffer and 2 μl of 1 M $MnCl_2$ in MnP vials). All groups were maintained under magnetic stirring, at room temperature and light protected for 60 days.

2.4. Characterizations

The hydrodynamic size, polydispersity and surface charge of the pre-dispersed nanomaterials were measured by DLS (Zetasizer Lab, Malvern Panalytical). A Quanta 250 FEG (FEI) microscope equipped with a retractable scanning transmission electron microscopy (STEM) detector working at a voltage of 30 KeV in brightfield STEM mode was employed for the electron microscopy observation of the dispersed nanomaterials. The sample solutions were dropped on a copper grid (Formvar film 300 Mesh, Cu from Electron Microscopy Sciences) and dried under ambient environment. The weight loss of the carbon materials under different temperatures was measured by TGA (STARe TGA 1, Mettler Toledo) with a ramp of 10 °C/min from 30 °C to 900 °C, under N_2 flow rate at 50 mL/min, depositing the samples on platinum pans. The atomic percentage and chemical state of C and O in the carbon materials were characterized by XPS (Kalpha, Thermo Scientific) with an Al anode as the X-ray source (1486 eV) at a basic chamber pressure of from 10^{-8} to

10^{-9} bar. The samples were deposited as powder and analysed three times with a spot size of 400 μm. The survey spectra were tested at a pass energy of 200 eV, with a step size of 1 eV, while high resolution spectra were recorded with the pass energy of 50 eV and the step size of 0.1 eV. The average value of scans for survey and high-resolution spectra were 10 and 30, respectively, and a flood gun was turned on during analysis. The presence of defects of the carbon materials was tested by Raman spectroscopy (inVia, Renishaw) equipped with a 514 nm laser and a Leica microscope, using × 100 objective lens. The samples were prepared by dropping 10 μL of the solution on a Si substrate (ThorLabs, USA) and they were irradiated with the laser power of 1 %. At least 3 accumulations each lasted 10 s were recorded, and finally 5 points were averaged.

3. Results and discussion

Aiming to assess the environmental degradability of the two types of selected commercial carbon materials (graphene and SWCNT), the first step was to analyse their structural characteristics. Indeed, the physicochemical properties of carbon nanomaterials often influence their stability and degradation.

3.1. Morphological characterization of the carbon materials

Firstly, the morphology of graphene and SWCNT was studied by STEM and DLS (Fig. 1). 2D graphene showed in STEM images sheet structures with various diameters. Although the size of graphene was not homogeneous, the diameters of these large sheets were still lower than 1 μm, indicating that the size of graphene was in nanometric scale (Fig. 1a). STEM images of SWCNT evidenced their tubular bundles with thin diameter and micron-sized length (Fig. 1b). These SWCNT displayed a lower contrast than graphene and were highly intertwined. The enzyme-mediated biodegradation of nanomaterials occurs essentially through the interaction between the enzymes and materials. Thus, good dispersion of nanomaterials facilitates sufficient contact with the enzymes, ensuring a complete progression of the degradation reaction. To study the dispersibility of the two carbon materials in the buffers of enzymatic reaction, DLS was performed (Fig. 1c and d). Similar mean values of hydrodynamic size (~600 nm) measured by DLS were obtained in all the groups containing graphene and SWCNT in PBS and PB buffer (Fig. 1c), indicating similar dispersion and stability of the nanomaterials in the different buffers. Combined with the results of STEM, the DLS data suggest that the materials form negligible aggregates in the buffers. Besides, the distribution plot also showed no aggregation of the carbon materials in these buffers (Fig. 1d).

3.2. Composition analysis of carbon materials

Next, the chemical composition of graphene and SWCNT was studied by TGA and XPS. Due to high strength of the C═C sp^2 covalent bonds, the thermostability of carbon materials is normally very high [19]. In our case, SWCNT showed only a slight weight loss at high temperature

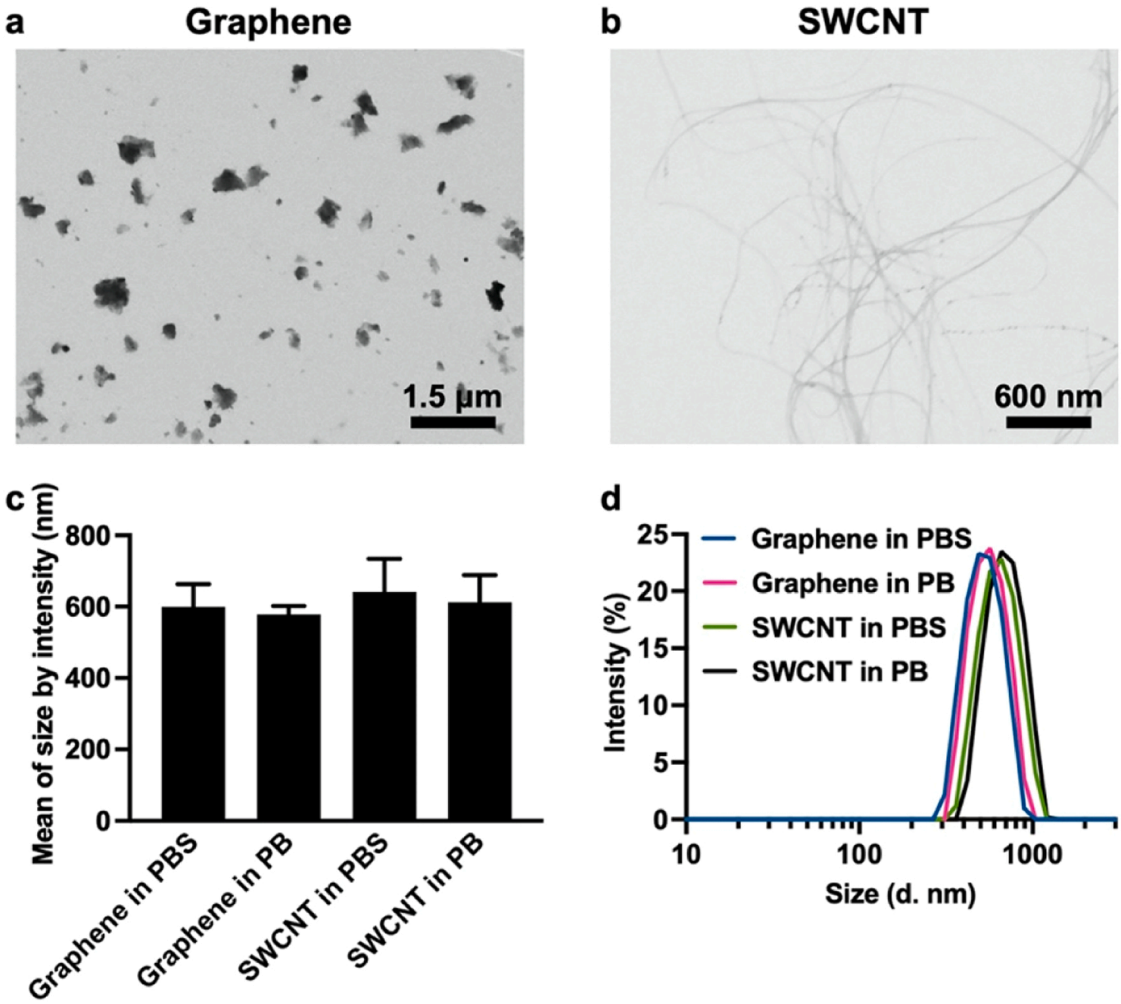

Fig. 1. Morphology characterization of graphene and SWCNT. STEM images of (a) graphene and (b) SWCNT. (c) Mean of size and (d) hydrodynamic size distribution of graphene and SWCNT in different buffers.

(<700 °C), exhibiting high thermostability (Fig. S1). Instead, around 30 % of weight reduction was observed for graphene, starting at ~300 °C (Fig. S1). This thermal decomposition temperature range can be attributed to the presence of some functional groups containing oxygen, such as -OH, -COOH or -C-O-C, indicating partial oxidation of this graphene [13].

Moreover, XPS was performed to gain insight into the elemental composition and the chemical states of the two carbon materials. Their carbon content was more than 90 % (Table 1). A higher oxygen content (~10 %) was observed in graphene compared to SWCNT, which had only 2.2 % of oxygen, probably coming from adsorbed CO_2 or O_2. The high oxygen content in graphene likely indicates the presence of oxygenated functional groups. The C 1s and O 1s peaks were clearly present in the survey spectra of graphene and SWCNT (Fig. 2a and d). In addition, the C 1s and O 1s high resolution spectra of two carbon materials were also analysed. Apart from the largest C═C/C-C peak at 284.8 eV, C-O bond at 286.3 eV was also observed in the high-resolution C 1s spectrum of graphene (Fig. 2b). Its presence was also confirmed in the O 1s high resolution spectrum at 533.5 eV (Fig. 2c). The intensity of the C═O peak in graphene was very low in comparison to C-O peak, suggesting that there is a tiny amount of carbonyl groups in this material. The intensity of the peaks of the oxygen-containing groups, such as C-O and O-C═O, was instead very low in the C 1s high-resolution spectrum of SWCNT in comparison to graphene (Fig. 2e). This is certainly due to the negligible amount of oxygen (only 2.2 %) observable in the survey spectrum of SWCNT (Fig. 2d and Table 1). However, the high-resolution O 1s spectrum of the nanotubes, evidenced the peaks relative to the C-O bond at 533.5 eV, the C═O bond at 531.5 eV and the O-C═O bond at 530.5 eV (Fig. 2f). All these results suggested a rather low level of oxidation in SWCNT, consistent with the conclusions obtained from TGA.

3.3. Raman analysis of carbon materials during the degradation

After investigating the morphology and the composition of graphene and SWCNT, we studied their enzymatic biodegradation. To simulate the natural enzyme condition, HRP (control group), EP 13 and MnP were selected, and their catalytic degradation ability on the two carbon materials were assessed. To align with the long-term and slow degradation process in the natural environment, the incubation of materials and enzymes lasted for a period of 60 days. After 60 days incubation, the degradation degree of the nanomaterials was measured by Raman spectroscopy. The Raman spectra can provide specific information about the defect level of the graphitic structures, which helps to estimate the degradation profile of these materials. The two typical peaks relative to the defected and the graphitic structures, namely the D and the G bands, are present at around 1350 and 1580 cm^{-1}, respectively. The ratio of the D and G band intensity (I_d/I_g) reveals the proportion of the defects in the structure. The Raman spectra of graphene were first measured (Fig. 3), evidencing a high intensity of the D band in each group, revealing that the graphene had inherently many defects. There was no increase on I_d/I_g after 60-day incubation in the absence of any enzymes (Fig. 3a and Table S1). This indicates that the buffer has no effect on the graphene degradation process. For the enzyme-treated graphene, higher D band intensity were measured after 60-day incubation, suggesting that the enzymatic treatment generated more defects on graphene (Fig. 3b-d). The values of I_d/I_g and their changes of the treated graphene are shown in Table S1. The increase of I_d/I_g reached 0.22 and 0.23 for HRP and EP 13 treatment, respectively, while after the MnP treatment, the value only increased by 0.12. These results suggested that HRP and EP 13 can effectively degrade graphene by introducing more defects. Even though, the degradation efficiency of MnP is significantly lower than the other two enzymes, it can still generate some defects on the graphitic structure, however longer degradation time is probably required. Similar results showing low increase of I_d/I_g values, but effective degradation observed by TEM were also reported on the degradation of single-layer or few-layer graphene by myeloperoxidase [14]. Next, the Raman spectra of SWCNT were tested (Fig. 4). In contrast to graphene, SWCNT showed a very small intensity of the D band, indicating more intact graphitic structure and higher stability. As expected, almost no changes in the D band and the ratios were observed after 60-day incubation, regardless of whether enzyme was added or not (Fig. 4 and Table S2). The results suggest that these three enzymes had no effect on the biodegradation of pristine SWCNT. Previous research also proved that the pristine SWCNT were more resistant to degradation by oxidative enzymes when compared to oxidized nanotubes [8].

Table 1
Atomic percentage of carbon and oxygen in carbon nanomaterials.

Materials	C	O
Graphene	90.1 %	9.9 %
SWCNT	97.8 %	2.2 %

The difference in the enzymatic degradation of these two carbon materials is closely related to their respective physicochemical properties. According to the results of TGA and XPS, graphene was found to have significantly more content of oxygen-containing functional groups, which can serve as the catalytic site of the enzymes, facilitating the degradation process. Moreover, the Raman spectra revealed that the graphene inherently contained a high number of defects. Both, these defects as well as the presence of oxygen-containing groups in graphene provided binding sites for the enzymes, enabling degradation to initiate easily. In addition, the 2D structure of graphene had a large interface for better interacting with the enzymes. All these factors made the graphene more prone to degradation than pristine SWCNT under the enzymatic treatment. This can be explained by the previous reports, which have demonstrated that the carboxylation is one of the essential conditions for the enzymatic biodegradation of SWCNT [1]. The hydrophilic carboxyl group facilitates the interaction with the enzymes, resulting in an effective Fenton-like reaction in the presence of H_2O_2 through the generation of hydroxyl or hydroperoxyl radicals on the surface of the material. However, for the pristine SWCNT with a more hydrophobic surface, the enzymes could be forced into a conformation in which their heme active site would be far away from the material, thus decreasing the catalytic efficiency.

3.4. TEM analysis of the carbon materials during the degradation

The structures of the two nanomaterials after the different treatments were also observed by TEM. As shown in Fig. 5, the structure of graphene without treatment showed no apparent changes between day 0 and day 60 (Fig. 5a and e). On the contrary, degraded structures with lots of hollows were observed in the peroxidase-treated graphene groups after 60-day incubation (Fig. 5b–d and f–h). The highly porous structure with less contrast was a typical morphology of the degraded graphene reported by the previous works, proving that the degradation occurred [14]. These results are consistent with the conclusions obtained from Raman spectra, confirming that the peroxidase-catalysed degradation occurred on the graphene. In addition, the structures of SWCNT after the different treatments were also observed by TEM (Fig. S2). As expected, no degraded structures were found in SWCNT. Star and his colleagues described in detail the morphology of the degraded CNTs (e.g., MWCNTs). The blurred boundaries of the nanotube walls were clearly observed in that CNTs, while in our case, the boundaries of the SWCNT are very clearly visible and intact, proving that no degradation happened [27]. Through TEM, the degraded graphene and intact SWCNT were visually observed, confirming the different degradation actions of the three enzymes on the two carbon materials.

4. Conclusions

The biodegradation of carbon materials in the environment helps to

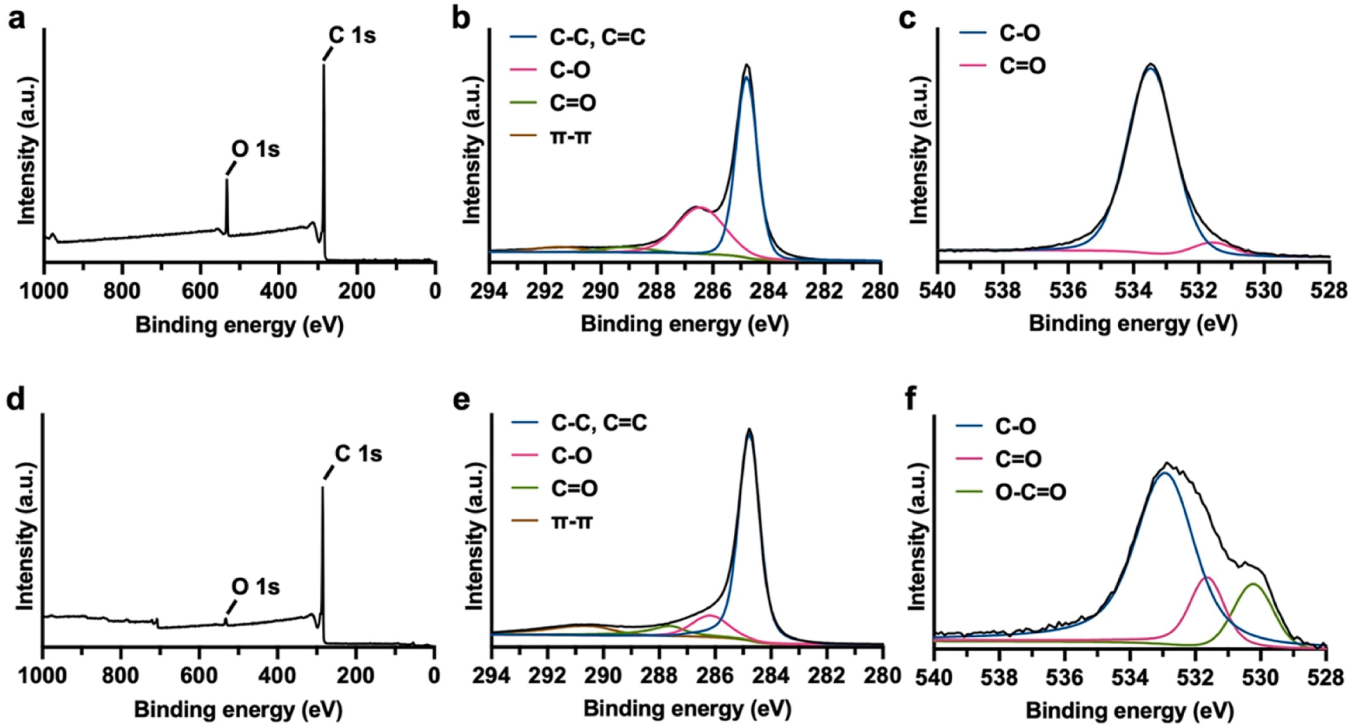

Fig. 2. XPS survey and high-resolution spectra of graphene and SWCNT. (a) Survey spectra, (b) C 1s and (c) O 1s high resolution spectra of graphene. (d) Survey spectra, (e) C 1s and (f) O 1s high resolution spectra of SWCNT.

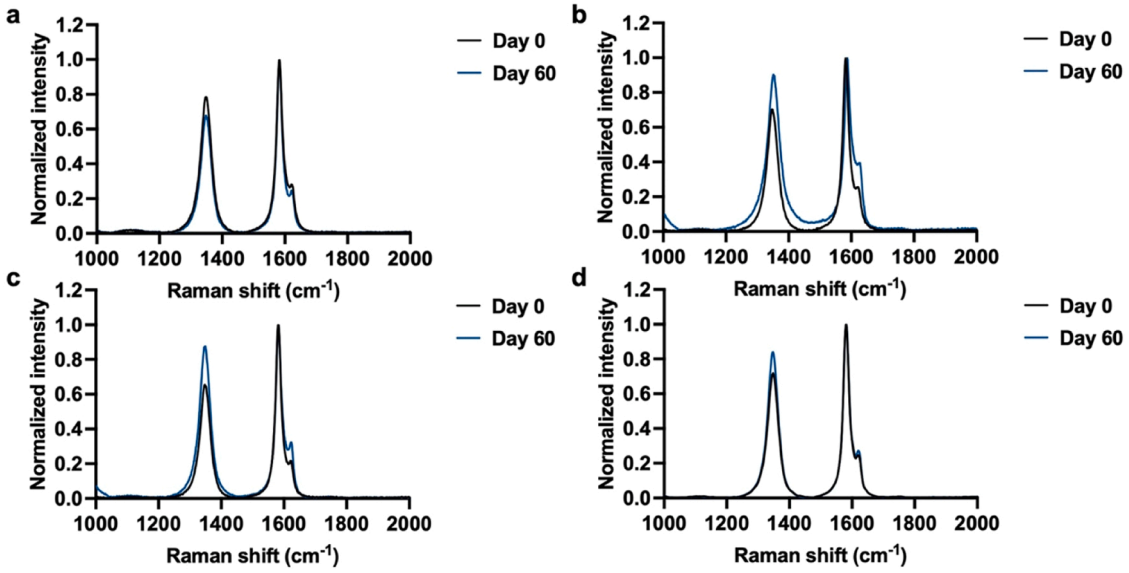

Fig. 3. Representative Raman spectra of graphene at day 0 and day 60 under different degradation conditions including (a) non treatment, (b) HRP treatment, (c) EP 13 treatment and (d) MnP treatment. The D band is located at ~1350 cm^{-1} and the G band is located at ~1580 cm^{-1}.

address concerns related to their potential applications and mitigate ecological as well as health impacts. In this study, the biodegradation effect of three peroxidases present in nature against different carbon materials was investigated. All three peroxidases have demonstrated the biodegradability of graphene in the presence of hydrogen peroxide. Among them, HRP and EP 13 were significantly more effective than MnP, generating more defects at the end of the treatment, according to Raman spectra. Moreover, the TEM images revealed degraded structures of graphene after 60 days of enzyme incubation, compared with the structures at day 0. On the contrary, no degradation of SWCNT was observed by Raman and TEM after the same enzymatic treatment. These results suggest that the carbon allotropes may have different impacts on the environment. Graphene is more easily removed by biodegradation, especially when it presents oxygenated functional groups, while pristine SWCNT may be more stable in the environment when released to the ecosystem. However, single-walled carbon nanotubes are not classified as hazards, and Safety Data Sheets according to the REACH Regulation, chemical safety assessment and exposure scenarios are available before use, allowing to consider and prevent the potential risks of accumulation and other ecological problems.

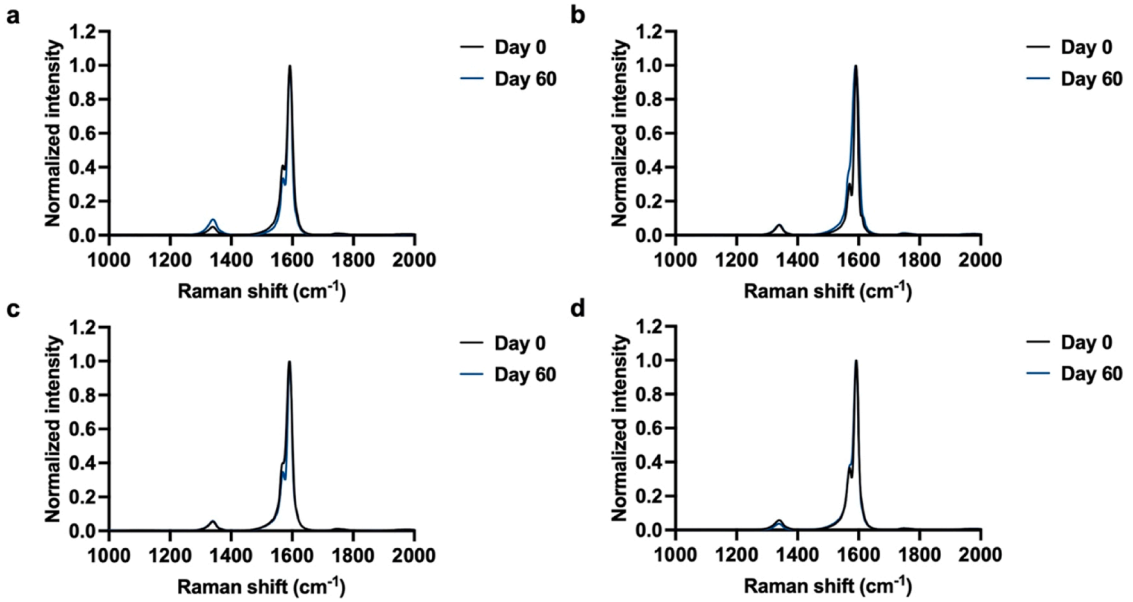

Fig. 4. Representative Raman spectra of SWCNT at day 0 and day 60 under different degradation conditions including (a) non treatment, (b) HRP treatment, (c) EP 13 treatment and (d) MnP treatment. The D band is located at ~1350 cm^{-1} and the G band is located at ~1580 cm^{-1}.

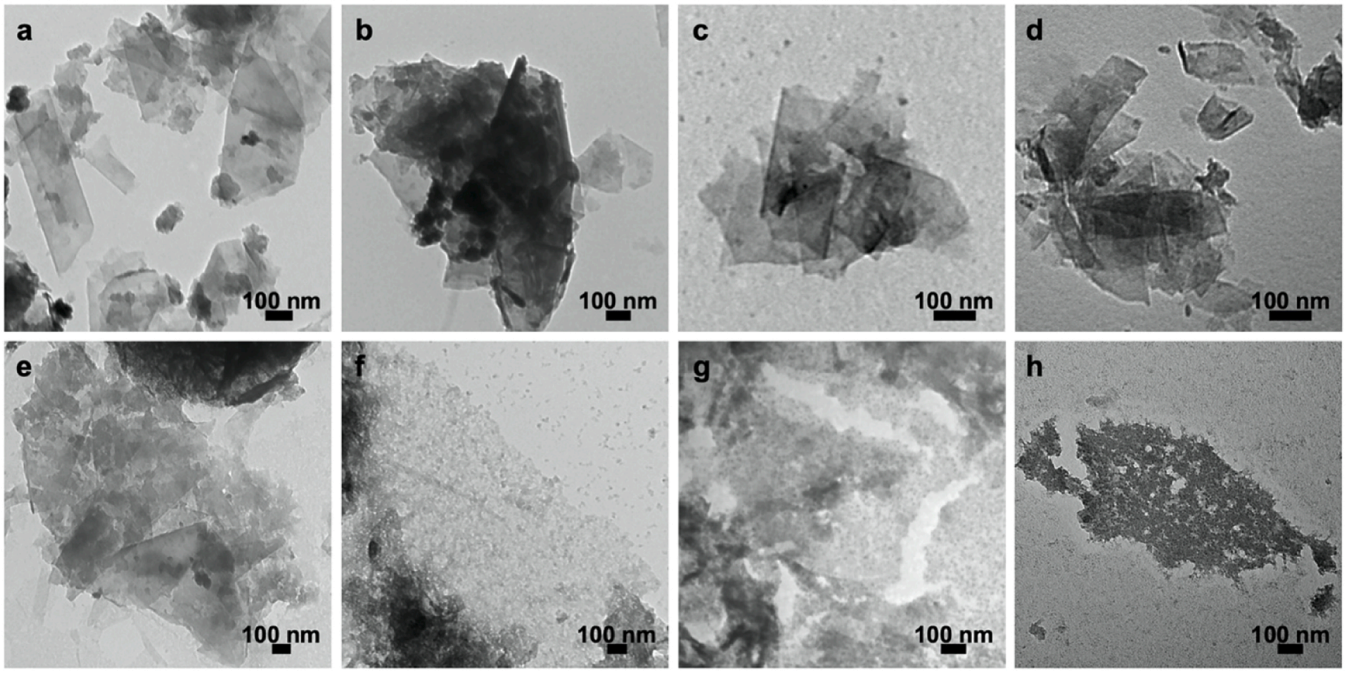

Fig. 5. Representative TEM images of graphene under different degradation conditions (enzyme treatment and non-treatment) at day 0 and day 60. Graphene: (a) without enzyme treatment, (b) with HRP treatment, (c) EP 13 treatment, and (d) MnP treatment at day 0. Graphene: (e) without enzyme treatment, (f) with HRP treatment, (g) EP 13 treatment, and (h) MnP treatment at day 60.

CRediT authorship contribution statement

Alberto Bianco: Writing – review & editing, Supervision, Funding acquisition, Conceptualization. **Tengfei Wang:** Writing – original draft, Investigation, Formal analysis, Data curation. **Nandita Dasgupta:** Investigation, Formal analysis, Data curation. **Álvaro Artiga:** Writing – review & editing, Investigation, Formal analysis, Data curation. **Carlos Rumbo:** Writing – review & editing, Supervision, Funding acquisition, Conceptualization. **Iwona Janica:** Writing – review & editing, Investigation, Formal analysis. **Juan Antonio Tamayo-Ramos:** Writing – review & editing, Supervision, Funding acquisition, Conceptualization.

Declaration of Competing Interest

The authors report no conflicts of interest.

Acknowledgments

This work is supported by funding from the European Union's Horizon 2020 Research and Innovation Programme under grant agreement No 953152 (DIAGONAL). The authors would like to thank Simone Ligi from Graphene-XT, and Gunther Van Kerckhove from OCSiAl Europe Sarl from providing the materials and critically reading the manuscript,

Cathy Royer from Plateforme Imagerie In Vitro de l'ITI Neurostra (CNRS UAR 3156, University of Strasbourg) for the sample fixation and TEM observations. N. D. would like to acknowledge the financial support received from Maria Zambrano aid modality financed by Next Generation EU.

Appendix A. Supporting information

Supplementary data associated with this article can be found in the online version at doi:10.1016/j.jece.2025.118671.

Data availability

Data will be made available on request.

References

[1] B.L. Allen, G.P. Kotchey, Y. Chen, N.V.K. Yanamala, J. Klein-Seetharaman, V. E. Kagan, A. Star, Mechanistic investigations of horseradish peroxidase-catalyzed degradation of single-walled carbon nanotubes, J. Am. Chem. Soc. 131 (2009) 17194–17205.
[2] S. Arora, B. Sharma, C. Srivastava, ZnCo-carbon nanotube composite coating with enhanced corrosion resistance behavior, Surf. Coat. Technol. 398 (2020) 126083.
[3] A. Artiga, H. Lin, A. Bianco, Interaction of industrial graphene and carbon nanotubes with human primary macrophages: assessment of nanotoxicity and immune responses, Carbon 223 (2024) 119024.
[4] M. Brazkova, R. Koleva, G. Angelova, H. Yemendzhiev, Ligninolytic enzymes in basidiomycetes and their application in xenobiotics degradation, BIO Web Conf. 45 (2022) 02009.
[5] C. Bussy, K.T. Al-Jamal, J. Boczkowski, S. Lanone, M. Prato, A. Bianco, K. Kostarelos, Microglia determine brain Region-Specific neurotoxic responses to chemically functionalized carbon nanotubes, ACS Nano 9 (2015) 7815–7830.
[6] K. Donaldson, C.A. Poland, F.A. Murphy, M. MacFarlane, T. Chernova, A. Schinwald, Pulmonary toxicity of carbon nanotubes and asbestos – similarities and differences, Adv. Drug Deliv. Rev. 65 (2013) 2078–2086.
[7] D. Elgrabli, W. Dachraoui, C. Ménard-Moyon, X. Liu, D. Bégin, S. Bégin-Colin, A. Bianco, F. Gazeau, D. Alloyeau, Carbon nanotube degradation in macrophages: live nanoscale monitoring and understanding of biological pathway, ACS Nano 9 (2015) 10113–10124.
[8] C. Farrera, K. Bhattacharya, B. Lazzaretto, F.T. Andon, K. Hultenby, G.P. Kotchey, A. Star, B. Fadeel, Extracellular entrapment and degradation of single-walled carbon nanotubes, Nanoscale 6 (2014) 6974–6983.
[9] I. García-Hevia, R. Soltani, J. González, O. Chaloin, C. Ménard-Moyon, A. Bianco, López, M. Fanarraga, Carbon nanotubes targeted to the tumor microenvironment inhibit metastasis in a preclinical model of melanoma, Bioact. Mater. 34 (2024) 237–247.
[10] A.K. Geim, K.S. Novoselov, The rise of graphene, Nat. Mater. 6 (2007) 183–191.
[11] C. Guilbaud-Chéreau, B. Dinesh, R. Schurhammer, D. Collin, A. Bianco, C. Ménard-Moyon, Protected amino Acid-Based hydrogels incorporating carbon nanomaterials for Near-Infrared Irradiation-Triggered drug release, ACS Appl. Mater. Interfaces 11 (2019) 13147–13157.
[12] G.P. Kotchey, B.L. Allen, H. Vedala, N. Yanamala, A.A. Kapralov, Y.Y. Tyurina, J. Klein-Seetharaman, V.E. Kagan, A. Star, The enzymatic oxidation of graphene oxide, ACS Nano 5 (2011) 2098–2108.
[13] S. Kundu, Y. Wang, W. Xia, M. Muhler, Thermal stability and reducibility of Oxygen-Containing functional groups on multiwalled carbon nanotube surfaces: a quantitative High-Resolution XPS and TPD/TPR study, J. Phys. Chem. C 112 (2008) 16869–16878.
[14] R. Kurapati, S.P. Mukherjee, C. Martín, G. Bepete, E. Vázquez, A. Pénicaud, B. Fadeel, A. Bianco, Degradation of Single-Layer and Few-Layer graphene by neutrophil myeloperoxidase, Angew. Chem. Int. Ed. 57 (2018) 11722–11727.
[15] K.-H. Liao, Y. Lin, C.W. Macosko, C.L. Haynes, Cytotoxicity of graphene oxide and graphene in human erythrocytes and skin fibroblasts, ACS Appl. Mater. Interfaces 3 (2011) 2607–2615.
[16] X.-W. Liu, Y.-X. Huang, X.-F. Sun, G.-P. Sheng, F. Zhao, S.-G. Wang, H.-Q. Yu, Conductive carbon nanotube hydrogel as a bioanode for enhanced microbial electrocatalysis, ACS Appl. Mater. Interfaces 6 (2014) 8158–8164.
[17] Z. Liu, J. Zhao, K. Lu, Z. Wang, L. Yin, H. Zheng, X. Wang, L. Mao, B. Xing, Biodegradation of graphene oxide by insects (Tenebrio molitor Larvae): role of the gut microbiome and enzymes, Environ. Sci. Technol. 56 (2022) 16737–16747.
[18] R. Madannejad, N. Shoaie, F. Jahanpeyma, M.H. Darvishi, M. Azimzadeh, H. Javadi, Toxicity of carbon-based nanomaterials: reviewing recent reports in medical and biological systems, Chem. Biol. Interact. 307 (2019) 206–222.
[19] M. Martincic, S. Sandoval, J. Oró-Solé, G. Tobías-Rossell, Thermal stability and purity of graphene and carbon nanotubes: key parameters for their thermogravimetric analysis (TGA), Nanomaterials 14 (2024) 1754.
[20] A. Paszczyński, V.-B. Huynh, R. Crawford, Enzymatic activities of an extracellular, manganese-dependent peroxidase from phanerochaete chrysosporium, FEMS Microbiol. Lett. 29 (1985) 37–41.
[21] Z. Peng, X. Liu, W. Zhang, Z. Zeng, Z. Liu, C. Zhang, Y. Liu, B. Shao, Q. Liang, W. Tang, X. Yuan, Advances in the application, toxicity and degradation of carbon nanomaterials in environment: a review, Environ. Int. 134 (2020) 105298.
[22] E.J. Petersen, L. Zhang, N.T. Mattison, D.M. O'Carroll, A.J. Whelton, N. Uddin, T. Nguyen, Q. Huang, T.B. Henry, R.D. Holbrook, K.L. Chen, Potential release pathways, environmental fate, and ecological risks of carbon nanotubes, Environ. Sci. Technol. 45 (2011) 9837–9856.
[23] S.S. Varghese, S. Lonkar, K.K. Singh, S. Swaminathan, A. Abdala, Recent advances in graphene based gas sensors, Sens. Actuators B Chem. 218 (2015) 160–183.
[24] S. Vranic, R. Kurapati, K. Kostarelos, A. Bianco, Biological and environmental degradation of two-dimensional materials, Nat. Rev. Chem. 9 (2025) 173–184.
[25] Y. Yang, A.M. Asiri, Z. Tang, D. Du, Y. Lin, Graphene based materials for biomedical applications, Mater. Today 16 (2013) 365–373.
[26] L. Zhang, E.J. Petersen, M.Y. Habteselassie, L. Mao, Q. Huang, Degradation of multiwall carbon nanotubes by bacteria, Environ. Pollut. 181 (2013) 335–339.
[27] Y. Zhao, B.L. Allen, A. Star, Enzymatic degradation of multiwalled carbon nanotubes, J. Phys. Chem. A 115 (2011) 9536–9544.
[28] J. Zhu, D. Yang, Z. Yin, Q. Yan, H. Zhang, Graphene and Graphene-Based materials for energy storage applications, Small 10 (2014) 3480–3498.